

TraFlow: Trajectory Distillation on Pre-Trained Rectified Flow

Zhangkai Wu¹

Xuhui Fan¹

Hongyu Wu²

Longbing Cao¹

^{1,2}Macquarie University, Australia
¹{zhangkai.wu, xuhui.fan, longbing.cao}@mq.edu.au
²hongyu.wu@students.mq.edu.au

Abstract

Majorities of distillation methods on pre-trained diffusion models or on pre-trained rectified flow, focus on either the distillation outputs or the trajectories between random noises and clean images to speed up sample generations from pre-trained models. In those trajectory-based distillation methods, consistency distillation requires the self-consistent trajectory projection to regulate the trajectory, which might avoid the common ODE approximation error while still be concerning about sampling efficiencies. At the same time, rectified flow distillations enforce straight trajectory for fast sampling, although an ODE solver is still required. In this work, we propose a trajectory distillation method, TraFlow, that enjoys the benefits of both and enables few-step generations. TraFlow adopts the settings of consistency trajectory models, and further enforces the properties of self-consistency and straightness throughout the entire trajectory. These two properties are pursued by reaching a balance with following three targets: (1) reconstruct the output from pre-trained models; (2) learn the amount of changes by pre-trained models; (3) satisfy the self-consistency over its trajectory. Extensive experimental results have shown the effectiveness of our proposed method.

1 INTRODUCTION

Diffusion models and rectified flows Ho et al. [2020], Song et al. [2021], Rombach et al. [2022], Poole et al. [2023], Esser et al. [2024] have become the dominant method in the synthesis and editing of high-quality images. However, its iterative design requires us to perform a large number of neural network evaluations to denoise from noise to high-quality data. To this end, distilling pre-trained diffusion models or

pre-trained rectified flows Salimans and Ho [2022], Wang et al. [2024], Yin et al. [2024b], Luo et al. [2024], Nguyen and Tran [2024], Yin et al. [2024a], Zhu et al. [2025], Sauer et al. [2025, 2024], Wang et al. [2023], Xu et al. [2024], Frans et al. [2025], Xie et al. [2024] which trained models to match their teacher model’s sample quality in fewer steps is one of the mainstream approaches.

Trajectory-based distillation methods constitute a representative class of distillation techniques applied to pre-trained diffusion models. These methods can be broadly categorized into consistency distillation Song et al. [2023], Kim et al. [2024], Lu and Song [2025] and rectified flow distillation Liu et al. [2023c], Zhu et al. [2025].

In consistency distillation, a trajectory projection function is introduced to model the incremental changes between two time steps. A fundamental requirement of this approach is the self-consistency property, which stipulates that the cumulative change over a large time step must be equivalent to the sum of changes over two smaller steps. By directly modeling these incremental changes, consistency distillation eliminates the need to solve an ordinary differential equation (ODE) during sample generation. However, despite avoiding ODE integration, multi-step generation remains necessary, as accurately modeling self-consistent trajectories presents a significant challenge.

Conversely, rectified flow distillation enforces a straight-line trajectory between random noise and ground-truth samples, thereby accelerating sample generation. By constraining the velocity field to approximate a linear trajectory, this approach mitigates approximation errors, allowing for simpler numerical integration methods such as Euler’s method. Consequently, fewer steps are required to generate high-quality samples. Nevertheless, since the learned velocity field is not strictly constant in practice, numerical integration using Euler’s method still introduces approximation errors.

In this paper, we propose TraFlow, a trajectory distillation method that may enjoy the benefits of both. The proposed TraFlow adopts the setting of consistency trajectory

model Kim et al. [2024]. In details, TraFlow considers three (self-)consistency distilling targets: (1) the self-consistency of the trajectory, which means two different previous points will be transited to the same value at a later time point; (2) the consistency of velocities, which refers to that the gradient of the distilling trajectory will be close to the amount of changes in the pre-trained model; (3) the consistency of trajectory outputs, which simply compares the trajectory outputs (at time step 0) between the distilled model and the pre-trained teacher model. These three targets regulate the distilled model from aspects of outputs, velocities, and trajectory itself.

The contributions of this paper can be summarised as: (1), we distill a pre-trained rectified flow into a time-step integrated model, which is easier than integrating the velocities; (2), in addition to the output difference loss, we introduce velocity approximation loss and output consistency loss; (4), we obtain state-of-the-art performance which uses smaller models to generate high-quality data with one-step.

2 PRELIMINARIES

Diffusion models Diffusion models (DMs) Ho et al. [2020] generate data by learning the score function of noise-corrupted images at multiple levels of noise. At each time step t , the *clean* image \mathbf{x}_0 is first diffused into a noisy image \mathbf{x}_t through a forward process defined as $\mathbf{x}_t := \alpha_t \mathbf{x}_0 + \sigma_t \epsilon$, $\epsilon \sim \mathcal{N}(\epsilon; \mathbf{0}, \mathbf{I})$, where α_t and σ_t^2 are the diffusion coefficient and variance, respectively. DMs then learn a neural network $\epsilon_\theta(\mathbf{x}_t, t)$ that matches the score of corrupted data $\mathbf{s}_{\text{real}}(\mathbf{x}_t) = \nabla_{\mathbf{x}_t} \log p_{t, \text{real}}(\mathbf{x}_t) = -\sigma_t^{-1}(\mathbf{x}_t - \alpha_t \mathbf{x}_0)$ by minimizing $\text{loss} \mathbb{E}_{t, \mathbf{x}_t} [\omega(t) \|\epsilon_\theta(\mathbf{x}_t, t) - \mathbf{s}_{\text{real}}(\mathbf{x}_t)\|^2]$, where $\omega(t)$ is a weighting function. Given a trained $\epsilon_\theta(\mathbf{x}_t, t)$, the data are generated through an iterative denoising process with T decreasing to 0.

Consistency Distillation As one of the trajectory distillation methods, consistency distillation (CM) Song et al. [2023] studies a consistency function $f_\phi(\mathbf{x}_t, t)$ mapping an noisy image \mathbf{x}_t back to the clean image \mathbf{x}_0 as $f_\phi(\mathbf{x}_t, t) = \mathbf{x}_0$. $f_\phi(\mathbf{x}_t, t)$ is usually parameterized as:

$$f_\phi(\mathbf{x}_t, t) = c_{\text{skip}}(t)\mathbf{x}_t + c_{\text{out}}(t)F_\phi(\mathbf{x}_t, t), \quad (1)$$

to satisfy the boundary condition at $t = 0$, where F_ϕ is the actual neural network to train, and $c_{\text{skip}}(t)$ and $c_{\text{out}}(t)$ are time-dependent factors such that $c_{\text{skip}}(0) = 1$, $c_{\text{out}}(0) = 0$.

While CM can be trained from scratch, a more popular choice for CM is to do distillation on pre-trained sampling trajectory, such as pre-trained DMs. In particular, the distillation objective function can be written as a distance metric between adjacent points as:

$$\mathcal{L}_{\text{CM}} = \mathbb{E}_i \left[\omega(t_i) d(\mathbf{f}_\phi(\mathbf{x}_{t_i+\Delta t}, t_i + \Delta t), \mathbf{f}_{\phi^-}(\hat{\mathbf{x}}_{t_i}^\theta, t_i)) \right], \quad (2)$$

where $d(\cdot, \cdot)$ is a metric function, ϕ^- is the exponential moving average (EMA) of the past values ϕ , and $\hat{\mathbf{x}}_{t_i}^\theta$ is obtained from pre-trained model as $\hat{\mathbf{x}}_{t_i}^\theta = \mathbf{x}_{t_i} - (t_i - t_{i+1})t_{i+1} \nabla_{\mathbf{x}_{t_{i+1}}} \log p_{t_{i+1}}(\mathbf{x}_{t_{i+1}})$

Consistency Trajectory Model (CTM) Kim et al. [2024] is introduced to minimize the accumulated estimation errors and discretization inaccuracies in multi-step consistency model sampling. While CM projects a noisy image \mathbf{x}_t to its clean image \mathbf{x}_0 , CTM extends it by designing a projection function which starts from time step t to its later step s ($s < t$) as:

$$f_\phi(\mathbf{x}_t, t, s) = s/t \cdot \mathbf{x}_t + (1 - s)/t \cdot F_\phi(\mathbf{x}_t, t, s). \quad (3)$$

where $F_\phi(\cdot)$ is the actual neural networks to be optimized. Equation (3) ensures $f_\phi(\mathbf{x}_t, t, s)$ satisfies the boundary condition when $f_\phi(\mathbf{x}_t, t, 1) = \mathbf{x}_1$.

Rectified flow methods Rectified flow methods Lipman et al. [2023], Liu et al. [2023b], Albergo et al. [2023] use ordinary differential equations (ODEs) to transit between two distributions $p_0(\cdot)$ and $p_1(\cdot)$. Letting $\mathbf{x}_0 \sim p_0(\mathbf{x}_0)$, $\mathbf{x}_1 \sim p_1(\mathbf{x}_1)$, rectified flows define a linear interpolation as $\mathbf{x}_t = t\mathbf{x}_1 + (1 - t)\mathbf{x}_0$, $0 \leq t \leq 1$. The model training may be achieved by:

$$\theta = \arg \min_{\theta} \int \mathbb{E} [\|\mathbf{x}_1 - \mathbf{x}_0\| - \mathbf{v}_\theta(\mathbf{x}_t, t)]^2 dt \quad (4)$$

$$\hat{\mathbf{x}}_0 = \mathbf{x}_1 + \int_1^0 \mathbf{v}_\theta(\mathbf{x}_t, t) dt.$$

Generating new image \mathbf{x}_0 from a white noise ϵ may follow the Ordinary Differential Equations (ODEs) as:

$$d\mathbf{x}_t = \mathbf{v}(\mathbf{x}_t, t) dt, t \in [0, 1] \quad (5)$$

With the ground-truth *velocity* setting as $d\mathbf{x}_t/dt = \mathbf{x}_1 - \mathbf{x}_0$, the trained $\mathbf{v}(\mathbf{x}_t, t)$ is expected to approximate the straight direction from \mathbf{x}_1 to $\mathbf{x}_0 = \epsilon$. As a result, rectified flows may use fewer steps than diffusion models to generate high-quality data.

There have been a few explorations on distilling a pre-trained rectified flow. InstaFlow Liu et al. [2023c], Zhu et al. [2025] proposes a direct distillation method which use one neural network to approximate the learned velocity's integration over the whole time. FlowDreamer Li et al. [2025] adopts score distillation sampling method to distill learned velocities.

3 METHODOLOGIES

The proposed Trajectory Distillation Flows (TraFlow) aim to distill a pre-trained rectified flow $\mathbf{v}(\mathbf{x}_t, t)$ Esser et al. [2024] into a ‘‘one-step’’ data generator $G_\phi(\mathbf{x}_1, 1, 0)$, $\mathbf{x}_1 \sim \mathcal{N}(\mathbf{0}, \mathbf{I})$. This generator $G_\phi(\mathbf{x}_1, 1, 0)$ is expected to produce high-quality data without time-consuming iterative sampling procedures.

Table 1: Different objective functions in distilling pre-trained rectified flows

Methods	Reflow	InstaFlow
Objective function	$\mathbb{E}_{\mathbf{x}_1 \sim \pi_1} \left[\int_0^1 \left\ \mathbf{v}_\phi(\mathbf{x}_t, t) - \int_0^1 \mathbf{v}(\mathbf{x}_r, r) dr \right\ ^2 dt \right]$	$\mathbb{E}_{\mathbf{x}_1 \sim \pi_1} \left[\left\ \mathbf{v}_\phi(\mathbf{x}_1, 1) - \int_0^1 \mathbf{v}(\mathbf{x}_r, r) dr \right\ ^2 \right]$
Methods	FlowDreamer	TraFlow
Objective function	$\mathbb{E}_{\mathbf{x}_1 \sim \pi_1} \left[\left\ \mathbf{v}_\phi(\mathbf{x}_t, t) - \mathbf{v}(\mathbf{x}_t, t) \right\ ^2 \right]$	$\mathbb{E}_{\mathbf{x}_1 \sim \pi_1} \left[\left\ \frac{\partial G_\phi(\mathbf{x}_1, 1, t)}{\partial t} - \int_0^1 \mathbf{v}(\mathbf{x}_r, r) dr \right\ ^2 \right]$

Given the pre-trained rectified flow $\mathbf{v}(\mathbf{x}_t, t)$, the clean image \mathbf{x}_0 can be obtained by solving the ODEs as $\hat{\mathbf{x}}_0 = \text{ODE}[\mathbf{v}](\mathbf{x}_1) = \mathbf{x}_1 + \int_1^0 \mathbf{v}(\mathbf{x}_s, s) ds$. Integration $\int_1^0 \mathbf{v}(\mathbf{x}_s, s) ds$ can be approximated using methods such as Euler forward method $\int_1^0 \mathbf{v}(\mathbf{x}_s, s) ds = \sum_{k=1}^K \mathbf{v}(\mathbf{x}_{t_k}, t_k) \Delta t_k$, where $t_1 = 0 < t_2 < \dots < t_K < t_{K+1} = 1$ represents the time steps taken to estimate the image. It is noted that such approximations may result in numerical errors.

Similarly to \mathbf{x}_0 , the intermediate variable \mathbf{x}_t may be estimated as $\mathbf{x}_t = (1-t)\hat{\mathbf{x}}_0 + t\mathbf{x}_1 = \mathbf{x}_1 - (1-t) \int_1^0 \mathbf{v}(\mathbf{x}_r, r) dr$, or $\mathbf{x}_t = \mathbf{x}_1 + \int_1^t \mathbf{v}(\mathbf{x}_r, r) dr$. For example, we may approximate $\int_t^1 \mathbf{v}(\mathbf{x}_r, r) dr$ as $\int_t^1 \mathbf{v}(\mathbf{x}_r, r) dr \approx \mathbf{v}(\mathbf{x}_1, 1)(1-t)/2 + \mathbf{v}(\mathbf{x}_{\frac{1+t}{2}}, \frac{1+t}{2})(1-t)/2$.

3.1 FORMULATING TRAFLOW

We use $G_\phi(\mathbf{x}_t, t, s)$ to denote TraFlow, which takes current time step t , its state \mathbf{x}_t , and the terminating time step s as inputs. $G_\phi(\mathbf{x}_t, t, s)$ is assumed to produce its state at time step s as $\hat{\mathbf{x}}_s := G_\phi(\mathbf{x}_t, t, s)$. Since it needs to satisfy the boundary condition of $G_\phi(\mathbf{x}_1, 1, 1) = \mathbf{x}_1$, we may formulate it as:

$$G_\phi(\mathbf{x}_t, t, s) = \frac{s}{t} \mathbf{x}_t + (1 - \frac{s}{t}) g_\phi(\mathbf{x}_t, t, s) \quad (6)$$

In this way, $g_\phi(\mathbf{x}_t, t, s)$ would be unconstrained, and the neural network structure can be used to describe $g_\phi()$.

In fact, assume TraFlow's state \mathbf{x}_s follows a velocity of $\boldsymbol{\mu}(\mathbf{x}_r, r)$, $G_\phi(\mathbf{x}_t, t, s)$ can be understood as an integration of $\boldsymbol{\mu}(\mathbf{x}_t, t)$, which is:

$$\mathbf{x}_s = \mathbf{x}_t + \int_t^s \boldsymbol{\mu}(\mathbf{x}_r, r) dr \quad (7)$$

In the following parts, we describe the three regulators that refine the trajectory of our TraFlow. These regulators are from the perspectives of output, velocity and trajectory.

3.2 MAIN COMPONENTS OF TRAFLOW

Output reconstruction We first regulate TraFlow to produce outputs similar to the teacher pre-trained model. Following Liu et al. [2023c], Zhu et al. [2025], we may formulate the output reconstruction loss as a root mean square error (RMSE) between the two outputs at time step 0:

$$\mathcal{L}_{\text{output}} = \mathbb{E}_{\mathbf{x}_1 \sim \pi_1} [\|G_\phi(\mathbf{x}_1, 1, 0) - \hat{\mathbf{x}}_0\|^2] \quad (8)$$

where $G_\phi(\mathbf{x}_1, 1, 0)$ directly transits random noise \mathbf{x}_1 at time step 1 to outputs at time step 0. By minimizing $\mathcal{L}_{\text{output}}$, TraFlow learns to compress the mapping from a random noise \mathbf{x}_1 to the pre-trained rectified flow $\mathbf{v}(\mathbf{x}_t, t)$'s estimated sample $\hat{\mathbf{x}}_0$ in one step.

Velocity approximation In addition to reconstructing output, we consider the differences of velocities between TraFlow and the pre-trained rectified flow, which is:

$$\mathcal{L}_{\text{vel}} = \mathbb{E}_{\mathbf{x}_1, t} \left[\left\| \lim_{\Delta t \rightarrow 0} \frac{G_\phi(\mathbf{x}_t, t, t + \Delta t) - G_\phi(\mathbf{x}_t, t, t)}{\Delta t} - \left(\hat{\mathbf{x}}_0 - \mathbf{x}_1 \right) \right\|^2 \right] \quad (9)$$

Minimizing Equation (9) helps to regulate the trajectory's velocity such that the velocity at any time step t can approximate the amount of changes from $t = 1$ to $t = 0$.

It is noted that this velocity approximation is different from the reflow mechanism. These two approximations are based on different inputs. More specifically, reflow takes the time step t and its current state \mathbf{x}_t as inputs, whereas our proposed velocity approximation is fed with the time step t and state at previous time step.

Minimizing Equation (9) approximates the velocities between the distilled and pre-trained models. In particular, we may use auto-differentiation of $G_\phi(\mathbf{x}_1, 1, t)$ to compare the velocity estimated in the pre-trained model. This is much faster and computational convenient than comparing the integration.

Output consistency Inspired from Consistency model Song et al. [2023] and Shortcut model Frans et al. [2025], we

attach a self-consistency property of the proposed TraFlow, which means that the projecting terminal of trajectory are the same given we have evaluated in the middle way as $G_\phi(\mathbf{x}_t, t, s) = G_\phi(\hat{\mathbf{x}}_{t+d}, t+d, s)$, $d = (s-t)/2$. We have two options as $\hat{\mathbf{x}}_{t+d} = G_\phi(\mathbf{x}_t, t, t+d)$, or $\hat{\mathbf{x}}_{t+d} = \mathbf{x}_t + \int_t^{t+d} \mathbf{v}(\mathbf{x}_r, r)dr$.

As a result, the loss regarding the consistency of output can be defined as:

$$\mathcal{L}_{\text{con}} = \mathbb{E}_{\mathbf{x}_1 \sim \pi_1, s, t} [\|G_\phi(\mathbf{x}_t, t, s) - G_\phi(\hat{\mathbf{x}}_{t+d}, t+d, s)\|^2] \quad (10)$$

Alternatively, we may adopt the soft consistency matching loss Kim et al. [2024] as:

$$G_\phi(\mathbf{x}_t, t, s) \approx G_{\text{sg}(\phi)}(\mathbf{x}_t + \int_t^s \mathbf{v}(\mathbf{x}_r, r)dr, u, s) \quad (11)$$

Objective function The objective function may be written as:

$$\mathcal{L} = \mathcal{L}_{\text{output}} + \lambda_{\text{vel}} \mathcal{L}_{\text{vel}} + \lambda_{\text{con}} \mathcal{L}_{\text{con}}. \quad (12)$$

where λ_{vel} and λ_{con} are the weights for \mathcal{L}_{vel} and \mathcal{L}_{con} , respectively.

3.3 SAMPLING

Algorithm 1 Sampling procedure of TraFlow

Input: Trained TraFlow $G_\phi(\mathbf{x}_t, t, s)$, pre-defined sampling steps $t_N = 1 > t_{N-1} > \dots > t_0 = 0$

Output: $\hat{\mathbf{x}}_{0,1}$

- 1: Start from $\mathbf{x}_{t_N} \sim \pi_1$
 - 2: **for** $n = N, N-1, \dots, 1$ **do**
 - 3: $\hat{\mathbf{x}}_{t_{n-1}} = G_\phi(\hat{\mathbf{x}}_{t_n}, t_n, t_{n-1})$
 - 4: **end for**
-

3.4 CONNECTIONS TO OTHER DISTILLATION METHODS

Our proposed TraFlow has deep connections to existing distillation methods.

TraFlow uses the same model structure as the consistency trajectory model (CTM) Kim et al. [2024]. The CTM mainly optimise the self-consistency loss to optimize the distilled model. However, the CTM does not consider the output reconstruction loss or the velocity, whereas the velocity may lead to straight trajectory which can help reduce the number of steps to generate samples.

Boot Gu et al. [2023] also considers the velocity alignment with the pre-trained model, by comparing the gradient of function.

InstaFlow Liu et al. [2023c] and SlimFlow Zhu et al. [2025] focus on output reconstruction. As velocity and self-consistency are not regularized, the trajectory is not well defined, which may result in unstable generation.

Shortcut model Frans et al. [2025] regulates the velocity behavior and self-consistent trajectories. As it estimates velocity, an approximated ODE solver is still needed.

Table 2: Symbols and their descriptions in training TraFlow.

Notion	Description
ϕ	Generator parameters
ψ	Discriminator parameters
\mathbf{t}	Current time step ($\mathbf{t} \in [0, 1]$)
\mathbf{s}	Target time step for state projection
N	Number of steps/evaluations
π_0	Data distribution at $\mathbf{t} = 0$
π_1	Noise distribution at $\mathbf{t} = 1$
g	Residual function within G_ϕ
G	Distilled generator function
\mathbf{z}	variable from $\mathcal{N}(\mathbf{0}, \mathbf{I})$

4 RELATED WORKS

Pre-trained diffusion distillation methods have emerged as a powerful strategy to alleviate the significant computational burden inherent in diffusion models, which traditionally require a large number of function evaluations to produce high-quality samples. By compressing the iterative denoising process into far fewer steps, these techniques not only expedite sample generation but also make it feasible to deploy such models in low-resource environments. In this work, we systematically categorize these distillation approaches into three major groups based on their underlying objectives and operational paradigms.

Output Reconstruction Based: These methods aim to minimize the discrepancy between the outputs of the teacher (i.e., the pre-trained diffusion model) and the student model by directly reconstructing the image outputs. Some approaches, such as Progressive Distillation Salimans and Ho [2022], Berthelot et al. [2023], focus on aligning the output values by enforcing a close correspondence between the denoising steps of the teacher and student. Other methods, for instance SDS and its variants Poole et al. [2023], Wang et al. [2024], Yin et al. [2024b,a], concentrate on matching the output distributions to preserve the statistical characteristics of the generated images. Additionally, certain works operate in a one-step denoising image space Lukoianov et al. [2024], Karras et al. [2022], allowing for the direct generation of high-quality images from a single function evaluation, while others employ Fisher divergence objectives Zhou et al. [2024a, 2025] to more rigorously align the gradients of the score functions. Together, these techniques

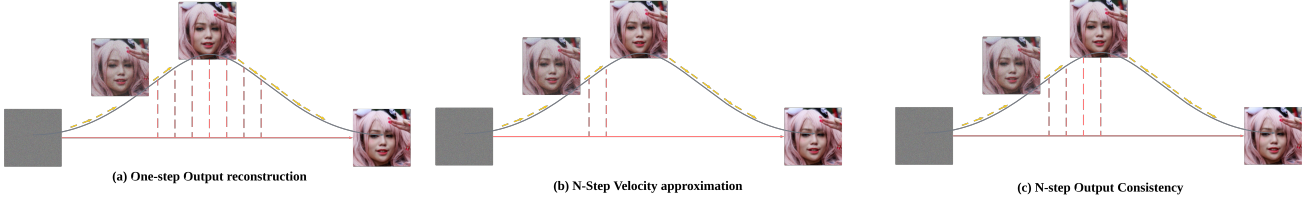
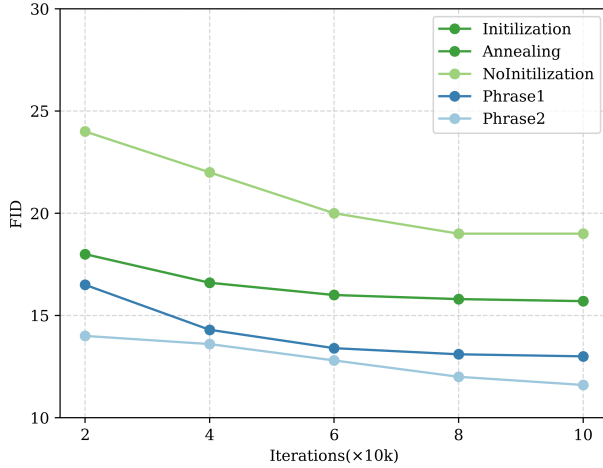
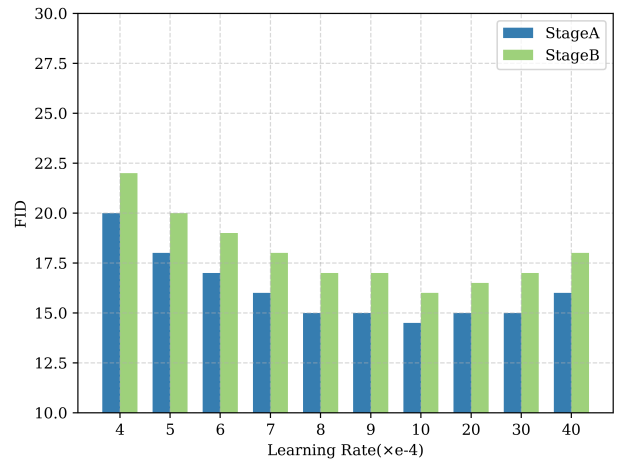


Figure 1: Visualisations of our TraFlow . Grey arrows represent the trajectories of pre-trained models, whereas yellow arrows correspond to the trajectories of the distillation models and the pink arrows correspond to the one step generation. We can see that in the panel, we randomly choose $N = \{0, \frac{1}{4}, \frac{1}{2}, 1\}$. Each yellow dot can show the velocity in the trajtorcy model and the shadow part is the approximated integration approximated in our TraFlow. We show three stages in approximation the one-way trajectory for one-step generation (a); the velocity approximation for N-way generation (b); the output consistency for N-way generation (c).

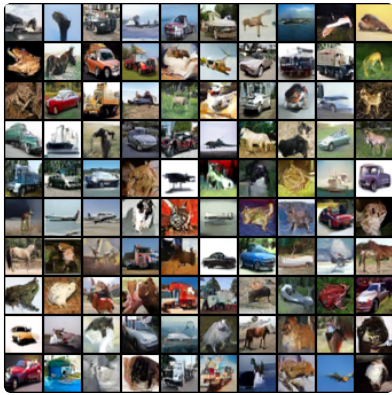


(a) Convergence in different Initialization Paradims

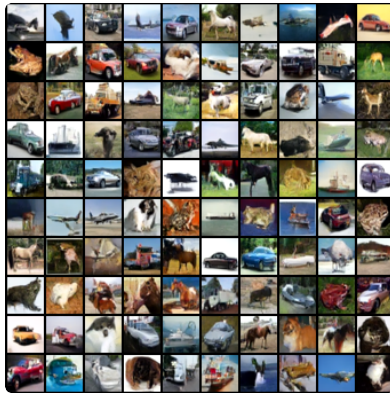


(b) Convergence in different Learning Rates

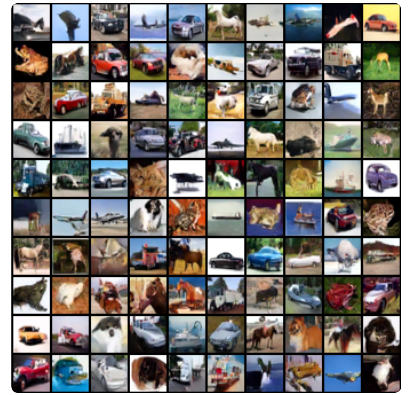
Figure 2: Training curves of training stages (a) and initialization(b).



(a) 1-Step



(b) 2-Step



(c) 4-Step

Figure 3: N -step Generation by our 3M TraFlow in 1, 2, 4 evaluation times, on CIFAR-10 32×32 image scale, using pre-trained Annealing 1-Rectified Flow as the teacher model.

effectively reduce the number of sampling steps required while maintaining the fidelity of the generated outputs.

Trajectory Distillation Based: Instead of concentrating solely on the final output, trajectory-based methods focus

on the entire denoising path—from the initial random noise to the eventual clean image. By distilling the full trajectory, these approaches ensure that the student model replicates not only the end result but also the dynamic behavior of

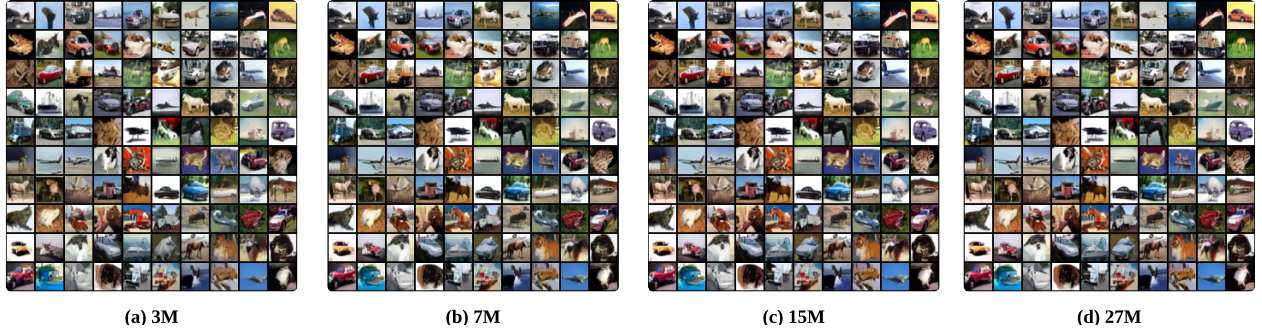


Figure 4: One step generation by our TraFlow in distilled model parameter varying from $\{3M, 7M, 15M, 27M\}$ on CIFAR-10 32×32 image scale, using pre-trained Annealing 1-Rectified Flow as the teacher model.

the teacher model throughout the diffusion process. Consistency distillation techniques Song et al. [2023], Kim et al. [2024], Lu and Song [2025] emphasize the self-consistency of the denoising trajectory, ensuring stable and accurate progression across different time steps. In contrast, rectified flow distillation methods such as InstaFlow and SlimFlow Liu et al. [2023c], Zhu et al. [2025] focus on producing a straighter, more direct trajectory, thereby mitigating the accumulation of approximation errors that typically arise from curved paths. Moreover, recent studies have demonstrated that integrating consistency modeling directly into rectified flows Frans et al. [2025] can further enhance the fidelity of the generated trajectories, effectively combining the strengths of both approaches.

Adversarial Distillation Based: A third category of distillation methods leverages adversarial learning to refine the student model’s output distribution. By incorporating an adversarial loss—often implemented via a pre-trained classifier or discriminator—these methods drive the student model to more closely approximate the target distribution provided by the teacher. Notably, works such as Sauer et al. [2024, 2025] have successfully employed this strategy to achieve competitive performance with significantly fewer sampling steps. The adversarial framework not only enhances the perceptual quality of the generated images but also provides a flexible plug-and-play mechanism that can complement other distillation strategies.

5 EXPERIMENT

5.1 EXPERIMENTAL SETUP

Notations We list the notation to train our TraFlow, specify the training parameters and data in teacher, student models. Refer to Table 2 for more information.

Datasets For fair comparison, We evaluate TraFlow on traditional real-world datasets, CIFAR-10, and extend our model on large scale datasets, FFQH-64 and ImageNet. Further details regarding these datasets can be found in Ta-

ble 10.

Pre-trained Models We initialized our trajectory model $G_\phi(\mathbf{x}_t, t, s)$ with open-source pre-trained velocity checkpoints $V_\theta(\mathbf{x}_t, t)$, and subsequently distilled it into an N -step model. Specifically, for the CIFAR-10 dataset, we distilled the model from the EDM and 1-Rectified Flow, follow by Zhu et al. [2025]. We choose EDM in Kim et al. [2024] and ADM Albergo et al. [2023] as the teacher model respectively for ImageNet and FFHQ-64 dataset.

Model Architecture To ensure fair comparisons across datasets, we adopt different model architectures that follow the design choices in Kim et al. [2024], Song et al. [2023], Zhu et al. [2025]. Specifically, for the CIFAR-10 dataset we use the Noise Conditioned Score Networks (NCSN++) architecture in Karras et al. [2022], for ImageNet we employ the Ablated Diffusion Model (ADM) architecture as detailed in Dhariwal and Nichol [2021]. We compare in Table 8 w.r.t. ResNetBlock, AttentionBlocks and SDE function corresponding to their specific U-Net design.

Training Hyperparameters We follow the optimization argument from SlimFlow Zhu et al. [2025]. Table 9 shows the optimization hyperparameters.

Evaluation Metrics. We assess TraFlow for unconditioned image generation using Precision and Recall Kynkäänniemi et al. [2019], the Inception Score (IS) Salimans et al. [2016], and the Fréchet Inception Distance (FID) Heusel et al. [2017]. We also report parameter counts, FLOPs and MACs to illustrate the distilled model’s efficiency. Additional details can be found in Appendix A.2.

Time Efficiency We assess the time efficiency of TraFlow across various loss functions by measuring both the evaluation time of G and the performance of the ODE solver. Table 3 summarizes the throughput results (imgs/sec./GPU).

5.2 CONVERGENCE OF TRAINING TRAFLOW MODEL

Since we employ a velocity model $v_\theta(\mathbf{x}_t, t)$ as the teacher to distill a generator model $g_\phi(\mathbf{x}_t, t, s)$ as the student, the training process encounters two challenges. First, the net-

Table 3: Time Efficiency (imgs/sec./H100) of TraFlow with different loss functions per datasets. (All values are approximate estimates)

	E.q. 8	E.q. 9	E.q. 10
CIFAR-10	400	400	100
ImageNet	400	400	100
FFHQ-64	160	160	20

work must learn to transition from velocity estimation to generator output; second, the teacher model provides limited support for learning the intermediate time step s .

To address the first knowledge transmission challenge, we adopt a two-stage training strategy. Initially, we train a generator-based consistency model $g_\phi(\cdot|t)$ to guide the network in transitioning from learning the velocity at time t to learning the generator at time t (i.e., training Eq. 10). Subsequently, we perform sample reconstruction in the image space while simultaneously conducting imitation learning for the velocity (i.e., training Eqs. 8 and 9. In Figure 2 (a), we compare two training schemes—one where Eqs. 8, 9, and 10 are trained jointly, and another where Eq. 10 is trained first followed by Eqs. 8 and 9—and report the evolution of FID over iterations.

For the second challenge, note that different teacher models support different input formats. Unlike the ADM model, the EDM model does not support conditional generation (it accepts only the sample at time t and the time t itself). Therefore, we override the EDM U-Net module by encoding s using the time encoding for t , which is then inserted into the ResNet and attention modules. Moreover, we reuse the initialization of the t module for training our model. Figure 2(b) compares the FID evolution over iterations when training TraFlow with and without this initialization.

5.3 N -STEP GENERATION FOR DISTILLED MODELS

In this section, we show the effectiveness of our TraFlow in N -step generation, varying various parameter scales. We compare the generation quality among models of different sizes under different Numbers of Function Evaluations (NFE) Lu et al. [2022], which is the number of calls $V_\phi(\cdot)/g_\theta(\cdot)$ to the velocity/trajectory models.

By specifying the depth and kernel size in ResNet and Attention Module from U-Net framework in student Models $g_\phi(\cdot)$, We distill several smaller TraFlow from teacher models. Simultaneously, training TraFlow in Eq. 10 can contain the consistency trajectory in generation N -step samples, we can specify the ODE solver to report the N -step generation.

32×32 Datasets We evaluated the generation performance of our distilled models with varying sizes across different

datasets. By leveraging the differences in ResNet and Attention modules within the U-Net architecture, we can distill student models with fewer parameters tailored to the teacher model, as detailed in Table 9.

Table 4 reports the performance of our models on the CIFAR-10 dataset. For the teacher models, we selected EDM and 2-Rectiflow to distill models of various sizes, and we also present generation performance under different step counts.

64×64 Datasets Furthermore, Tables 5, 6 reports the performance of our models on 64×64 datasets. Following the approach outlined in Zhu et al. [2025], we employed the 2-Rectified model as the teacher model and distilled 7, 15, 28, 32MB models varying the neural network units in U-Net specified in Table 9.

Figure 3 demonstrates the N -step generation quality achieved by our TraFlow, showing that our trajectory model can generate high-quality samples with only a few function evaluations—even achieving effective results in a single step. The distilled model significantly accelerates sampling while maintaining excellent sample quality. Furthermore, Figure 4 illustrates that our distilled TraFlow, across varying parameter sizes {3M, 7M, 15M, 27M }, is capable of 1-step generation without compromising sample quality.

5.4 ABLATION STUDIES

In this chapter, we analyze the component selection in training our TraFlow. Specifically, we investigate whether the quality of generated samples from our trained distilled model is influenced by (i) whether our student network, conditioned on (\mathbf{x}_t, t, s) , is initialized from the teacher network conditioned on (\mathbf{x}_t, t) ; (ii) the choice of the pre-trained teacher model; (iii) the divergence function adopted in Eq. 8; (iv) the velocity correction loss in Eq. 9; (v) the consistency loss in Eq. 10; and (vi) the number of evaluations in the Euler solver for the consistency loss in Eq. 10. We report the corresponding ablation results via FID in Table 7.

6 CONCLUSION

In this paper, we presented TraFlow, a trajectory distillation framework that effectively compresses pre-trained rectified flows into a compact generator. Our approach simultaneously aligns the output, velocity, and self-consistency of the distilled model with the teacher model. Extensive experiments on CIFAR-10, CelebA, FFHQ-64, and ImageNet demonstrate that TraFlow achieves competitive generation quality with significantly fewer sampling steps and reduced computational cost. This work highlights the potential of trajectory distillation for accelerating generative models and paves the way for future research on efficient and high-quality image synthesis.

Table 4: Comparison of different DMs by N -step generation performance on CIFAR-10 at corresponding model scales. Bold red numbers indicate distilled models’ parameters. We report sample quality (FID and IS) for model sizes (4MB, 7MB, 15MB, 28MB) across N -step generation ($N = 1, 2, \text{and } 4$) with a shadow background.

NFE↓	Methods	Model Size			Generation Quality	
		FLOPs (G)	MACs (G)	Params (M)	FID↓	IS↑
50	DDIM Song et al. [2020]	12.2	6.1	35.7	4.67	—
20	DDIM Song et al. [2020]	12.2	6.1	35.7	6.84	—
10	DDIM Song et al. [2020]	12.2	6.1	35.7	8.23	—
10	DPM-solver-2 Lu et al. [2022]	12.2	6.1	35.7	5.94	—
10	DPM-solver-fast Lu et al. [2022]	12.2	6.1	35.7	4.70	—
10	3-DEIS Zhang and Chen [2022]	20.6	10.3	61.8	4.17	—
2	PD Salimans and Ho [2022]	41.2	20.6	55.7	5.58	9.05
2	CD Song et al. [2023]	41.2	20.6	55.7	2.93	9.75
2	CT Song et al. [2023]	41.2	20.6	55.7	5.83	8.85
4	TraFlow-16M	7.4	3.7	15.7	5	—
4	TraFlow-28M	13.2	6.6	27.9	4	—
2	TraFlow-16M	7.4	3.7	15.7	5	—
2	TraFlow-28M	13.2	6.6	27.9	4	—
1	1-Rectified Flow (+Distill) Liu et al. [2023a]	20.6	10.3	61.8	378 (6.18)	1.13 (9.08)
1	2-Rectified Flow (+Distill) Liu et al. [2023a]	20.6	10.3	61.8	12.21 (4.85)	8.08 (9.01)
1	3-Rectified Flow (+Distill) Liu et al. [2023a]	20.6	10.3	61.8	8.15 (5.21)	8.47 (8.79)
1	TraFlow-16M	7.4	3.7	15.7	5.8	—
1	TraFlow-28M	13.2	6.6	27.9	4.5	—

Table 5: Comparison of different DMs by N -step generation performance on FFHQ-64 at corresponding model scales. Bold red numbers indicate distilled models’ parameters. We report sample quality (FID and IS) for model sizes (16MB) across N -step generation ($N = 1, 2, 4$) with a shadow background.

NFE↓	Methods	Model Size			Generation Quality	
		FLOPs	MACs	Params	FID↓	Prec.↑
79	EDM Karras et al. [2022]	167.9	82.7	55.7	2.47	—
10	DDIM Song et al. [2020]	167.9	82.7	55.7	18.30	—
5	AMED-Solver Zhou et al. [2024b]	167.9	82.7	55.7	12.54	—
2	TraFlow-16M	30.4	14.8	15.7	7	—
1	Boot Gu et al. [2023]	52.1	25.3	66.9	9.00	—
1	SlimFlow Zhu et al. [2025]	53.8	26.3	27.9	7.21	—
1	SlimFlow Zhu et al. [2025]	30.4	14.8	15.7	7.70	—
1	TraFlow-16M	30.4	14.8	15.7	7	—

Table 6: Comparison of different DMs by N -step generation performance on ImageNet at corresponding model scales. Bold red numbers indicate distilled models’ parameters. We report sample quality (FID and IS) for smaller model sizes (81MB) across N -step generation ($N = 1, 2, 4$) with a shadow background.

NFE↓	Methods	Model Size			Generation Quality	
		FLOPs	MACs	Params	FID↓	Prec.↑
250	ADM Karras et al. [2022]	219.4	103.4	295.9	2.07	0.74
79	EDM Dhariwal and Nichol [2021]	219.4	103.4	295.9	2.44	0.71
2	PD Salimans and Ho [2022]	219.4	103.4	295.9	15.39	0.59
2	CD Song et al. [2023]	219.4	103.4	295.9	4.70	0.69
2	CT Song et al. [2023]	219.4	103.4	295.9	11.10	0.69
2	TraFlow-81M	67.8	31.0	80.7	12	—
1	CD Song et al. [2023]	219.4	103.4	295.9	6.20	0.68
1	CT Song et al. [2023]	219.4	103.4	295.9	13.00	0.71
1	SlimFlow Zhu et al. [2025]	67.8	31.0	80.7	12.34	—
1	TraFlow-81M	67.8	31.0	80.7	12	—

References

- Michael S Albergo, Nicholas M Boffi, and Eric Vanden-Eijnden. Stochastic Interpolants: A Unifying Framework for Flows and Diffusions. *arXiv preprint arXiv:2303.08797*, 2023.
- David Berthelot, Arnaud Autef, Jierui Lin, Dian Ang Yap, Shuangfei Zhai, Siyuan Hu, Daniel Zheng, Walter Talbott, and Eric Gu. Tract: Denoising Diffusion Models with Transitive Closure Time-Distillation. *arXiv preprint arXiv:2303.04248*, 2023.
- Prafulla Dhariwal and Alexander Nichol. Diffusion Models Beat GANs on Image Synthesis. *NeurIPS*, 2021.
- Patrick Esser, Sumith Kulal, Andreas Blattmann, Rahim Entezari, Jonas Müller, Harry Saini, Yam Levi, Dominik Lorenz, Axel Sauer, Frederic Boesel, et al. Scaling Rectified Flow Transformers for High-Resolution Image Synthesis. *ICML*, 2024.
- Kevin Frans, Danijar Hafner, Sergey Levine, and Pieter Abbeel. One Step Diffusion via Shortcut Models. *ICLR*, 2025.
- Jiatao Gu, Shuangfei Zhai, Yizhe Zhang, Lingjie Liu, and Joshua M Susskind. Boot: Data-free Distillation of Denoising Diffusion Models with Bootstrapping. *ICML*, 2023.
- Martin Heusel, Hubert Ramsauer, Thomas Unterthiner, Bernhard Nessler, and Sepp Hochreiter. Gans Trained by a Two Time-Scale Update Rule Converge to a Local Nash Equilibrium. *NeurIPS*, 2017.

Table 7: Ablation study w.r.t initialization from, choices of teacher model, divergence and loss function, and approximation time in Euler Solver of 3MB TraFlow on CIFAR-10.

Initialize from θ	Teacher Model	Divergence \mathcal{D}	$E.q. 8$	$E.q. 9$	$E.q. 10$	FID↓
+	EDM	L2	+	-	-	16
-	EDM	L2	+	-	-	15
-	2-Rectified Flow	L2	+	-	-	14
-	2-Rectified Flow	LPIPS	+	-	-	13
-	2-Rectified Flow	LPIPS	+	+	-	13
-	2-Rectified Flow	LPIPS	+	+	+	13
-	2-Rectified Flow	LPIPS	+	+	2	13

- Jonathan Ho, Ajay Jain, and Pieter Abbeel. Denoising Diffusion Probabilistic Models. *NeurIPS*, 2020.
- Tero Karras, Miika Aittala, Timo Aila, and Samuli Laine. Elucidating the Design Space of Diffusion-based Generative Models. *NeurIPS*, 2022.
- Dongjun Kim, Chieh-Hsin Lai, Wei-Hsiang Liao, Naoki Murata, Yuhta Takida, Toshimitsu Uesaka, Yutong He, Yuki Mitsufuji, and Stefano Ermon. Consistency Trajectory Models: Learning Probability Flow ODE Trajectory of Diffusion. *ICLR*, 2024.
- Tuomas Kynkäänniemi, Tero Karras, Samuli Laine, Jaakko Lehtinen, and Timo Aila. Improved Precision and Recall Metric for Assessing Generative Models. *NeurIPS*, 2019.
- Hangyu Li, Xiangxiang Chu, Dingyuan Shi, and Wang Lin. Flowdreamer: Exploring High Fidelity Text-to-3D Denoising via Rectified Flow. *ICLR*, 2025.
- Yaron Lipman, Ricky TQ Chen, Heli Ben-Hamu, Maximilian Nickel, and Matt Le. Flow Matching for Generative Modeling. *ICLR*, 2023.
- Xingchao Liu, Chengyue Gong, and Qiang Liu. Flow Straight and Fast: Learning to Generate and Transfer Data with Rectified Flow. *ICLR*, 2023a.
- Xingchao Liu, Chengyue Gong, and qiang liu. Flow Straight and Fast: Learning to Generate and Transfer Data with Rectified Flow. *ICLR*, 2023b.
- Xingchao Liu, Xiwen Zhang, Jianzhu Ma, Jian Peng, et al. InstafLOW: One Step is enough for High-quality Diffusion-based Text-to-Image Generation. *ICLR*, 2023c.
- Cheng Lu and Yang Song. Simplifying, Stabilizing and Scaling Continuous-time Consistency Models. *ICLR*, 2025.
- Cheng Lu, Yuhao Zhou, Fan Bao, Jianfei Chen, Chongxuan Li, and Jun Zhu. Dpm-Solver: A Fast ODE Solver for Diffusion Probabilistic Model Sampling in around 10 Steps. *NeurIPS*, 2022.
- Artem Lukoianov, Haitz Sáez de Ocáriz Borde, Kristjan Greenewald, Vitor Campagnolo Guizilini, Timur Bagautdinov, Vincent Sitzmann, and Justin Solomon. Score Distillation via Reparametrized DDIM. *arXiv preprint arXiv:2405.15891*, 2024.
- Weijian Luo, Tianyang Hu, Shifeng Zhang, Jiacheng Sun, Zhenguo Li, and Zhihua Zhang. Diff-Instruct: A Universal Approach for Transferring Knowledge From Pre-trained Diffusion Models. *NeurIPS*, 2024.
- Thuan Hoang Nguyen and Anh Tran. Swiftbrush: One-Step Text-to-Image Diffusion Model with Variational Score Distillation. *CVPR*, 2024.
- Ben Poole, Ajay Jain, Jonathan T Barron, and Ben Mildenhall. Dreamfusion: Text-to-3D using 2D Diffusion. *ICLR*, 2023.
- Robin Rombach, Andreas Blattmann, Dominik Lorenz, Patrick Esser, and Björn Ommer. High-resolution Image Synthesis with Latent Diffusion Models. *CVPR*, 2022.
- Olga Russakovsky, Jia Deng, Hao Su, Jonathan Krause, Sanjeev Satheesh, Sean Ma, Zhiheng Huang, Andrej Karpathy, Aditya Khosla, Michael Bernstein, et al. Imagenet Large Scale Visual Recognition Challenge. *IJCV*, 2015.
- Tim Salimans and Jonathan Ho. Progressive Distillation for Fast Sampling of Diffusion Models. *ICLR*, 2022.
- Tim Salimans, Ian Goodfellow, Wojciech Zaremba, Vicki Cheung, Alec Radford, and Xi Chen. Improved Techniques for Training GANs. *NeurIPS*, 2016.
- Axel Sauer, Frederic Boesel, Tim Dockhorn, Andreas Blattmann, Patrick Esser, and Robin Rombach. Fast High-Resolution Image Synthesis with Latent Adversarial Diffusion Distillation. *SIGGRAPH*, 2024.
- Axel Sauer, Dominik Lorenz, Andreas Blattmann, and Robin Rombach. Adversarial Diffusion Distillation. *ECCV*, 2025.
- Jiaming Song, Chenlin Meng, and Stefano Ermon. Denoising Diffusion Implicit Models. *arXiv preprint arXiv:2010.02502*, 2020.

- Yang Song, Jascha Sohl-Dickstein, Diederik P Kingma, Abhishek Kumar, Stefano Ermon, and Ben Poole. Score-based Generative Modeling through Stochastic Differential Equations. *ICLR*, 2021.
- Yang Song, Prafulla Dhariwal, Mark Chen, and Ilya Sutskever. Consistency Models. *ICML*, 2023.
- Christian Szegedy, Vincent Vanhoucke, Sergey Ioffe, Jon Shlens, and Zbigniew Wojna. Rethinking the Inception Architecture for Computer Vision. *CVPR*, 2016.
- Zhendong Wang, Huangjie Zheng, Pengcheng He, Weizhu Chen, and Mingyuan Zhou. Diffusion-GAN: Training GANs with Diffusion. *ICLR*, 2023.
- Zhengyi Wang, Cheng Lu, Yikai Wang, Fan Bao, Chongxuan Li, Hang Su, and Jun Zhu. Prolificdreamer: High-Fidelity and Diverse Text-to-3D Generation with Variational Score Distillation. *NeurIPS*, 2024.
- Sirui Xie, Zhisheng Xiao, Diederik P Kingma, Tingbo Hou, Ying Nian Wu, Kevin Patrick Murphy, Tim Salimans, Ben Poole, and Ruiqi Gao. Em Distillation for One-Step Diffusion Models. *NeurIPS*, 2024.
- Yanwu Xu, Yang Zhao, Zhisheng Xiao, and Tingbo Hou. UFOGen: You Forward Once Large Scale Text-to-Image Generation via Diffusion GANs. *CVPR*, 2024.
- Tianwei Yin, Michaël Gharbi, Taesung Park, Richard Zhang, Eli Shechtman, Fredo Durand, and William T Freeman. Improved Distribution Matching Distillation for Fast Image Synthesis. *NeurIPS*, 2024a.
- Tianwei Yin, Michaël Gharbi, Richard Zhang, Eli Shechtman, Fredo Durand, William T Freeman, and Taesung Park. One-Step Diffusion with Distribution Matching Distillation. *CVPR*, 2024b.
- Qinsheng Zhang and Yongxin Chen. Fast Sampling of Diffusion Models with Exponential Integrator. *arXiv preprint arXiv:2204.13902*, 2022.
- Mingyuan Zhou, Huangjie Zheng, Zhendong Wang, Mingzhang Yin, and Hai Huang. Score Identity Distillation: Exponentially Fast Distillation of Pretrained Diffusion Models for One-Step Generation. *ICML*, 2024a.
- Mingyuan Zhou, Huangjie Zheng, Yi Gu, Zhendong Wang, and Hai Huang. Adversarial Score identity Distillation: Rapidly Surpassing the Teacher in One Step. *ICLR*, 2025.
- Zhenyu Zhou, Defang Chen, Can Wang, and Chun Chen. Fast ODE-based Sampling for Diffusion Models in around 5 Steps. *CVPR*, 2024b.
- Yuanzhi Zhu, Xingchao Liu, and Qiang Liu. Slimflow: Training Smaller One-Step Diffusion Models with Rectified Flow. *ECCV*, 2025.

Title in Title Case (Supplementary Material)

Zhangkai Wu¹

Xuhui Fan¹

Hongyu Wu²

Longbing Cao¹

^{1,2}Macquarie University, Australia
¹{zhangkai.wu, xuhui.fan, longbing.cao}@mq.edu.au
²hongyu.wu@students.mq.edu.au

Table 8: U-Net Comparison employed in distilled models varing datasets.

Components	Functions	NCSN++ (CIFAR-10,FFHQ-64)	ADM (ImageNet)
ResNetBlock	Resampling filter	Bilinear	Box
	Noise embedding	Fourier	Positional
	Skip connections	Residual	-
	Residual blocks per resolution	4	3
AttentionBlock	Resolutions	16	32, 16, 8
	Heads	1	6–9–12
	Blocks in DownSampling	4	9
	Blocks in UpSampling	2	13
ScoreFunction	Vanillia forward SDE	VP	VE
	Denoise Condition	-	label

Table 9: Training configuration of TraFlow varying different model sizes on CIFAI-10.

	Hyperparameters	CIFAI-10 3M	CIFAI-10 7M	CIFAI-10 15M	CIFAI-10 28M
U-Net	Base channels	128	128	192	256
	Channel multipliers	1, 2, 2, 4	1, 2, 2, 4	1, 2, 4, 4	1, 2, 4, 4
	Attention resolution	16	16	8	8
	Blocks	2, 2, 2, 2	2, 2, 2, 2	2, 2, 2, 2	2, 2, 2, 2
Optimization	Learning rate $\times 10^4$	1.5	1.0	0.75	0.5
	Warm up	5k iterations	5k iterations	5k iterations	5k iterations
	Batch	64	64	64	64
	Images trained	50M	50M	50M	50M
	Optimizer	AdamW	AdamW	AdamW	AdamW
	Dataset flips	Enabled	Enabled	Enabled	Enabled
	Weight decay	0.01	0.01	0.01	0.01
	Dropout probability	0.1	0.1	0.1	0.1
	Mixed-Precision (FP16)	Enabled	Enabled	Enabled	Enabled
Score	ODE Solver	RK45	RK45	RK45	RK45
	EMA decay rate	0.999	0.999	0.999	0.999
	LR ramp-up (Mimg)	1	1	1	1
	EMA half-life (Mimg)	10	10	10	10

Table 10: Experimental Details of Datasets.

Data Shape	Dataset	Samples	Data Size
$(3 \times 32 \times 32)$	CIFAR-10	60K	160M
	CelebA	60K	160M
$(3 \times 64 \times 64)$	FFHQ-64	70K	2 GB
	ImageNet	1.2M	6 GB

A TECHNICAL DETAILS

A.1 DATASETS

CIFAR-10¹: This dataset contains 60,000 32×32 color images evenly distributed over 10 distinct classes (6,000 images per class). It is split into a training set of 50,000 images and a test set of 10,000 images, making it a standard benchmark in machine learning and computer vision.

FFHQ-64²: The original FFHQ dataset consists of 70,000 high-quality images at 1024×1024 resolution. It is not categorized into specific classes; rather, it is used for tasks like generative modeling of faces. For our experiments, we downscale the images to 64×64, maintaining the dataset’s focus on high-quality facial imagery without predefined class labels. The dataset is provided in LMDB format for efficient access and storage. Packaged files and usage instructions are available in an anonymous repository.

ImageNet³: ImageNet is one of the most influential benchmarks in computer vision. It comprises over 1.2 million training images and around 50,000 validation images, categorized into 1,000 diverse classes. The dataset’s vast scale and rich annotations have made it an essential resource for developing and evaluating deep learning models.

A.2 METRICS

Precision and Recall. Following the approach in Dhariwal and Nichol [2021], we obtain these two metrics by evaluating 10k real images and 10k synthesized images. In a pre-trained feature space, we use nearest neighbors to define the manifolds for both real and generated data. Precision indicates the fraction of generated samples that lie within the manifold of real data, whereas Recall measures the fraction of real data that falls within the manifold of generated samples. Since Precision is related to fidelity (how realistic the samples appear) and Recall is associated with diversity (how varied the samples are), both metrics complement each other.

Inception Score (IS). IS is influenced by both fidelity and diversity. We compute IS from the logits of a pre-trained Inception Network Szegedy et al. [2016] trained on ImageNet Russakovsky et al. [2015]. A high IS arises when the model classifies each sample with strong confidence and, collectively, covers multiple classes. However, when dealing with face datasets such as FFHQ or CelebA, the limited possibility of assigning samples to distinct categories (e.g., 26 classes) makes it hard to capture diversity, causing the IS to predominantly reflect fidelity. We measure IS with 10k generated images. For our implementation, we employ implement of Precision, Recall and and IS from ADM repository⁴.

FID. To evaluate Fréchet Inception Distance (FID), we approximate real and generated data as Gaussians in the Inception feature space and measure their Wasserstein distance, thus taking into account both fidelity and diversity. For our implementation, we adopt clean-FID⁵ to compute FID.

Parameter counts (B). We report the total number of parameters in the model in billions (B), counting of a neural network is determined by summing the learnable parameters. . The count is determined by summing all learnable weights (e.g., convolutional kernels, dense layer matrices) and biases. A higher parameter count may enable richer representation learning,

¹<https://www.cs.toronto.edu/~kriz/cifar.html>

²<https://github.com/NVlabs/ffhq-dataset>

³<http://www.image-net.org/>

⁴<https://github.com/openai/guided-diffusion>

⁵<https://github.com/GaParmar/clean-fid>

while a lower count suggests a compact architecture suitable for resource-constrained environments. For transformer-based models, we include all attention weights and feed-forward network parameters.

FLOPs. FLOPs quantify the total floating-point operations (additions and multiplications) required for a single forward pass of the model. For a convolutional layer with kernel size $H \times W$, FLOPs are calculated as:

$$\text{FLOPs} = 2 \times H \times W \times k^2 \times C_{\text{in}} \times C_{\text{out}}.$$

This metric captures the overall computational complexity and serves as an indicator of efficiency. Lower FLOP counts generally imply a more efficient model, which is crucial for real-time applications and deployment on resource-constrained devices.

MACs. Multiply-accumulate operations (MACs) provide a practical estimate of the model’s computational workload during inference. MACs measure fused multiply-add operations, which are commonly optimized as a single instruction in hardware (e.g., GPUs and TPUs). For the same convolutional layer, MACs are defined as:

$$\text{MACs} = H \times W \times k^2 \times C_{\text{in}} \times C_{\text{out}}.$$

MACs directly correlate with hardware efficiency, as modern accelerators often optimize for MAC throughput. We calculate MACs using the `calcflops` library⁶ and emphasize their relevance for deployment on edge devices.

⁶<https://github.com/MrYxJ/calculate-flops.pytorch>